29 June 2001

ELSEVIER

Chemical Physics Letters 341 (2001) 638–644

CHEMICAL PHYSICS LETTERS

www.elsevier.nl/locate/cplett

Absolute generalized oscillator strength profiles of Si 2p shape resonances in SiF_4

X.W. Fan, K.T. Leung *

Department of Chemistry, University of Waterloo, Waterloo, Ontario, Canada N2L 3G1

Received 8 March 2001; in final form 24 April 2001

Abstract

Absolute generalized oscillator strengths (GOSs) of the Si 2p shape resonances in silicon tetrafluoride (SiF_4) have been determined as functions of momentum transfer by angle-resolved electron energy loss spectroscopy at 2.5 keV impact energy. These GOS profiles reveal subtle details about the spectral nature of the underlying dipole-allowed Si $2p \rightarrow 2e$ and Si $2p \rightarrow 7t_2$ continuum transitions, particularly with respect to the pre-edge Si $2p \rightarrow 6a_1\sigma^*$ resonance. The GOS profiles of the Si 2p shape resonances in SiF_4 are compared with those of the corresponding S $2p \rightarrow 2t_{2g}$ and S $2p \rightarrow 4e_g$ resonances in SF_6.

As a gaseous electronics gas commonly encountered in silicon etching and related processing in the semiconductor industry, silicon tetrafluoride (SiF_4) represents one of the more relevant technological silicon compounds. SF_6 [1,2] and SiF_4 are two of the most popular model compounds for investigating the so-called 'caged' effects, as manifested most notably by intense well-defined resonance features in the respective S and Si 2p continuum regions of molecular photoabsorption. These continuum or shape resonances have continued to attract considerable theoretical and experimental attentions. Various models have been proposed to explain the underlying mechanisms for the enhancement in the cross-sections, which include inner-well quasi-bound states supported by ligand-induced centrifugal potential barriers, interactions with virtual molecular orbitals (MOs), delayed onsets of atomic p and d core-level cross-sections, and scattering of ejected core electrons from the ligands [3]. The electronic structure of the Si 2p shell in SiF_4 has been the subject of intense investigation by a variety of techniques, including photoabsorption [3–7] and small-angle electron scattering [8]. These studies have revealed two prominent features above the Si 2p edge that can generally be classified as shape resonances. Although there is general agreement in the assignment of the broad intense feature at ~133 eV to a shape resonance with a t_2 symmetry, the nature (symmetry) of the lower lying shape resonance at 117 eV is less definite and depending upon different calculations could be attributed to having either e or t_2 symmetry [3,9]. Our recent work has provided the first measurement of generalized oscillator strength (GOS) profiles for some of the more prominent features in the pre-ionization-edge valence and Si 2p regions of SiF_4 [10]. In the present work, we investigate the absolute GOS profiles of the two predominant post-edge resonances in the

* Corresponding author. Fax: +1-519-746-0435.
E-mail address: tong@uwaterloo.ca (K.T. Leung).

0009-2614/01/$ - see front matter
PII: S0009-2614(01)00532-2

Si 2p continuum region of SiF_4 and compare their spectral signatures with analogous shape resonances in other 'cage-like' molecules including CCl_4 [11] and SF_6 [1].

Lassettre and coworkers [12] have pioneered the use of angle-resolved electron energy loss spectroscopy (EELS) for precise absolute measurements of GOS, as a means to determine absolute dipole OSs by extrapolating the measured GOS profiles to the optical limit. Furthermore, the GOS profile (over an extended range of momentum transfer) of an individual transition at a particular energy loss can also be used to provide detailed 'mapping' of the overlap function between the initial-state and final-state wave functions in momentum space. The GOS profiles therefore represent important information that can be used to assist spectral assignments, theoretical modeling of the excited-state wave functions, and better understanding of the nature of underlying interactions for both dipole-allowed and non-dipole transitions [13]. Despite the lower energy resolution in high-energy electron scattering work relative to modern synchrotron-radiation photoabsorption studies, the development of angular sampling (i.e., measurement as a function of the scattering angle or momentum transfer) has opened up a new window into dipole forbidden phenomena that are not easily accessible by optical methods, particularly in the valence-shell region. In the case of inner shells, only a handful of GOS profiles have been reported and the references to these studies are given in a recent review by Leung [14]. The present work offers further 'benchmark' GOS measurements of resonance transitions in the inner shell of an important cage-like molecule.

The experimental technique and our angle-resolved EELS apparatus have been described in detail elsewhere [15]. Briefly, a collimated electron beam was crossed with a gas jet at 2.5 keV impact energy and the electrons scattered with an energy loss at a selected scattering angle (from the forward direction) were analyzed with standard electron optics. The scattering angle θ is related to the magnitude of the momentum transfer $\mathbf{K}(=\mathbf{k}_0-\mathbf{k})$ by $K^2=k_0^2+k^2-2k_0k\cos\theta$, where $\mathbf{k}_0$ and $\mathbf{k}$ are the momenta of the incident and scattered electrons, respectively. Angle-resolved EELS spectra of the sample gas introduced to the center of the collision cell (sample spectra) at a typical chamber pressure of $1\text{–}2\times10^{-5}$ Torr were collected over an extended energy loss range of 200 eV from $\theta=1.5°$ to 9.5° in steps of 0.5° sequentially in repetitive scans. A similar set of spectra (ambience spectra) was obtained under identical conditions with the sample gas introduced outside the collision cell. Contributions from the ambient gas were then removed by subtracting the respective ambience spectra from the sample spectra after appropriate normalization. The correction of the ambience contribution is crucial for obtaining precise GOS results especially for inner-shell transitions with low cross-sections. SiF_4 (99.99% purity) was purchased from Matheson and used without further purification. Our spectrometer was operated routinely with an energy resolution of 0.8 eV full width at half maximum and an angular resolution of 0.2° half-angle at 2.5 keV impact energy. The energy and angular scales have been calibrated by using standard procedures as discussed previously [2]. No geometrical correction was found to be necessary for the 'short' experimental angular range and the high-impact energy employed in the present work.

In the first Born approximation, the high-energy electron collision can be considered as a sudden, impulsive process. The intensity of the scattered electron with an energy loss E at a scattering angle θ is proportional to the differential cross-section $\mathrm{d}^2\sigma/\mathrm{d}\Omega\,\mathrm{d}E$, which can be converted to the differential GOS, $\mathrm{d}f(K,E)/\mathrm{d}E$, by using the Bethe–Born formula (in Rydberg atomic units) [16]:

$$\frac{\mathrm{d}f(K,E)}{\mathrm{d}E}=\frac{k_0}{k}K^2\frac{E}{4}\frac{\mathrm{d}^2\sigma}{\mathrm{d}\Omega\,\mathrm{d}E}, \tag{1}$$

where $\mathrm{d}\Omega$ corresponds to the detection solid angle. The GOS is defined as:

$$f(K,E)=\frac{E}{K^2}\left|\left\langle\Psi_n\left|\sum_{j=1}^{N}\exp(i\mathbf{K}\cdot\mathbf{r}_j)\right|\Psi_0\right\rangle\right|^2, \tag{2}$$

where Ψ_0 and Ψ_n are the (N-electron) electronic wave functions of the initial and final states respectively, and $\mathbf{r}_j$ is the position of the jth electron with respect to the center-of-mass of the target.

The GOS at any momentum transfer can be made absolute independently by using the Bethe-sum-rule [16]:

$$\int \frac{\mathrm{d}f(K,E)}{\mathrm{d}E}\,\mathrm{d}E = N, \tag{3}$$

where N is the total number of electrons in the target. In the Bethe-sum-rule normalization procedure, the intensity of the relative GOS obtained at a pre-selected momentum transfer is first numerically integrated over the sampling energy loss range of 100 eV. The remaining intensity of the valence-shell above 100 eV for SiF_4 is estimated by integration of a fitted function $B(E) = a/E^{1.5} + b/E^{2.5} + c/E^{3.5}$ from 100 eV to infinity, where the empirical constants a, b, and c are obtained by curve-fitting $B(E)$ to the experimental data in the separate E range 70–100 eV. The sum of these two integrated intensities is then normalized to the integrated oscillator strength of 3.34, which corresponds to the total number of valence-shell (32), plus an appropriate correction of the contribution due to Pauli-excluded transitions from other inner shells (1.4) [17,18].

SiF_4 is a 50-electron system with a T_d molecular symmetry. In accord with the photoelectron data [19,20], the single-electron configuration for the ground electronic state of SiF_4 can be written as:

$$\underbrace{1a_1^{\,2}}_{\text{Si 1s}}\ \underbrace{1t_2^{\,6}2a_1^{\,2}}_{\text{F 1s}}\ \underbrace{3a_1^{\,2}}_{\text{Si 2s}}\ \underbrace{2t_2^{\,6}}_{\text{Si 2p}}\quad \underbrace{4a_1^{\,2}3t_2^{\,6}}_{\text{inner-valence}}$$

$$\underbrace{5a_1^{\,2}4t_2^{\,6}1e^{\,4}5t_2^{\,6}1t_1^{\,6}\ (\text{HOMO})}_{\text{outer-valence orbitals}}\ \Big|\ \underbrace{6a_1^{\,0}\ (\text{LUMO})\ 6t_2^{\,0}2e^{0}7t_2^{\,0}}_{\text{unoccupied virtual orbitals}}$$

The vertical ionization potentials for the removal of the outer-valence MOs [20] and the energies for the main ionic states of the inner-valence orbitals [21], as well as the term values for the unoccupied virtual MOs and Rydberg orbitals have been summarized in our recent work [10]. Of relevance to the present work, simple MO calculations show that the two lowest unoccupied MOs (LUMOs), $6a_1$ and $6t_2$, are made up largely of antibonding σ^* overlaps between the Si 3s and F 2p orbitals, and between the Si 3p and F 2p orbitals, respectively. Transitions from the $2t_2$ (Si 2p) orbital to these virtual orbitals occur below the Si 2p ionization edge and are commonly referred as σ^* resonances. On the other hand, the remaining 2e and $7t_2$ virtual MOs are essentially non-bonding Si 3d orbitals. Transitions from the Si 2p orbital to these final-state orbitals take place above the Si 2p edge and they give rise to the shape resonances, all of which are dipole-allowed transitions because they behave in effect like atomic p → d transitions.

Fig. 1 shows selected absolute EELS spectra for the Si 2p region of SiF_4 at 1.5°, 3.0°, 4.5°, 6.0°, and 7.5°, which correspond, respectively, to momentum transfers of 0.46, 0.76, 1.10, 1.44, and 1.78 a.u.

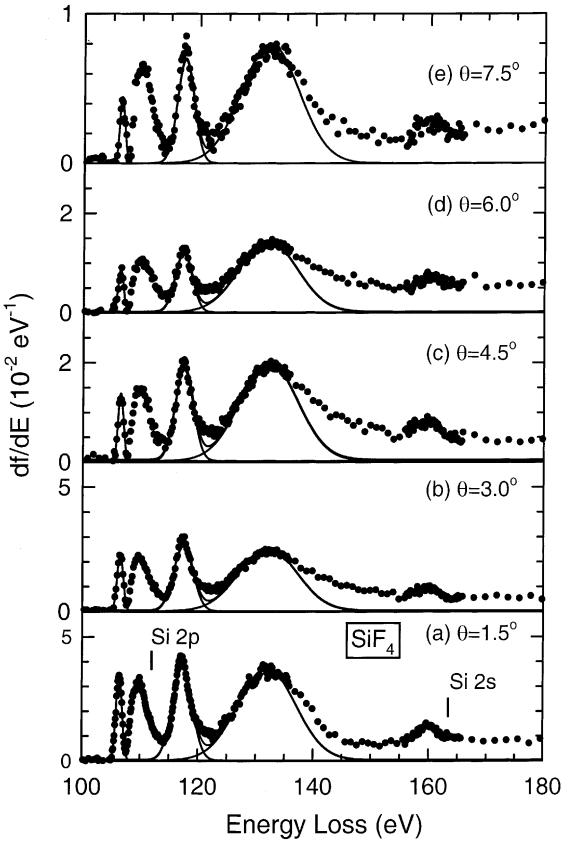

Fig. 1. Absolute angle-resolved electron energy loss spectra of the Si 2p shell in SiF_4 measured at 2.5 keV impact energy and (a) 1.5°, (b) 3.0°, (c) 4.5°, (d) 6.0°, and (e) 7.5°. Intensities arising from the valence shell have been removed from the background. Three Gaussian line-shapes with the appropriate line-widths are used to estimate the intensities of the Si 2p → $6a_1$, Si 2p → 2e, and Si 2p → $7t_2$ resonances at 106.4, 117.5, and 132.5 eV, respectively, in a curve-fitting procedure. The ionization potentials of Si $2p_{3/2}$, $2p_{1/2}$ and 2s are 111.7, 112.3, and 163.7 eV, respectively.

at 110 eV energy loss. The background from the valence-shell contribution has been appropriately removed from these inner-shell spectra, which are automatically normalized on an absolute scale because the entire set of EELS spectra (from valence-shell to 200 eV) was collected in a self-normalized fashion. As shown in our recent work [10], the overall intensity variation of our EELS spectrum with increasing scattering angle (Fig. 1) has been found to be consistent with the photoabsorption spectrum of Friedrich et al. [5] and the 'corrected' zero-angle EELS spectrum of Guo et al. [8] (as suggested by Olney et al. [22]). The characteristic reduction in the GOS with increasing scattering angle (momentum transfer) as depicted in Fig. 1 indicates the predominantly dipole-allowed nature of the spectral features in the Si 2p region. Briefly, an intense peak (doublet) at 106.4 eV, corresponding to the Si $2p\sigma^*$ resonance, and a broader band centered at 109.5 eV are found below the ionization edges of Si $2p_{3/2}$ at 111.7 eV and Si $2p_{1/2}$ at 112.3 eV in our spectrum. The broader band at 109.5 eV can be further resolved into several peaks (including individual spin–orbit components) [5,8,10], and the assignments of these inner-shell features have been discussed in more detail in our recent work [10]. Above the ionization edges, the prominent peak observed at 117.5 eV and the broad band centered at 132.5 eV cannot be resolved further even with a higher energy resolution [8]. The large natural line-widths of these shape resonances are characteristic of the inherently short lifetimes of these continuum states. The post-edge feature at 117.5 eV has been assigned as an e shape resonance associated with transitions to quasi-bound states in the continuum induced by the electronegative F ligands, while the band at 132.5 eV can be described as a t_2 shape resonance or alternatively an atomic-like delayed onset phenomenon [3,8].

The GOSs of the Si $2p\sigma^*$ resonance at 106.4 eV and the two Si 2p shape resonances at 117.5 and 132.5 eV are approximated by curve-fitting with Gaussian line-shapes, the spin–orbit energy splitting and natural line-widths of which are obtained from the photoabsorption spectrum of Friedrich et al. [5] and high-resolution zero-angle EELS spectrum of Guo et al. [8,22]. In the case of the t_2 shape resonance at 132.5 eV, the fit is somewhat limited because the experimental line-shape is evidently not symmetric and difficult to ascertain (Fig. 1). Fig. 2 shows the resulting GOS profiles of the three features, estimated from the areas under the respective Gaussian line-shapes. The gradual decrease with increasing momentum transfer from its maximum at zero momentum transfer in these GOS profiles is consistent with the spectral assignments that the Si 2p (formally $2t_2$ in the MO notation) features are dominated by dipole-allowed transitions. Despite the similarity, the GOS profiles of the two Si 2p shape resonances (Fig. 2b,c) are noticeably broader than that of the Si $2p\sigma^*$ resonance (Fig. 2a).

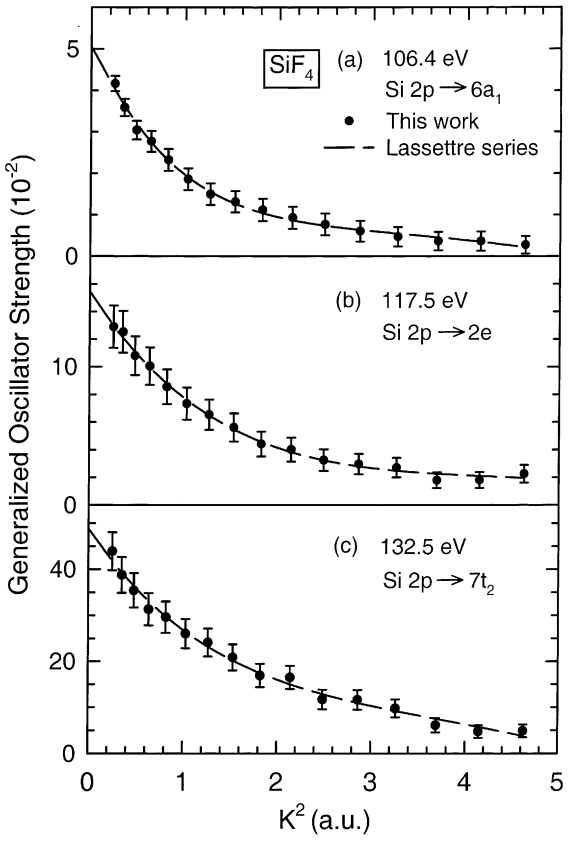

Fig. 2. Absolute GOS as a function of momentum transfer (K) squared for the Si 2p features at (a) 106.4, (b) 117.5, and (c) 132.5 eV in SiF_4. The dashed lines correspond to semiempirical fits using the Lassettre series.

For angle-dependent studies that involve finite momentum transfers, Lassettre and coworkers [23–25] have shown that the GOS for a bound-state excitation can be expanded as an even power series of K (the so-called Lassettre series), which we have previously extended to include transitions to continuum states, as follows [1]:

$$f(K,E) = \frac{1}{(1+x)^6}\sum_{n=0}^{m} f_n\left(\frac{x}{1+x}\right)^n; \quad 2 \leqslant m \leqslant 5, \tag{4}$$

where $x = K^2/(\sqrt{2I} + \sqrt{2|I-W|})^2$, I is the ionization potential, and W is the excitation energy of the transition. We have fitted the GOS profiles (Fig. 2) semiempirically using the above modified form of the Lassettre series up to $m = 3$ and derived the dipole OS f_0 and other f_n coefficients shown in Table 1. The integer m is chosen according to the amount of available data points and the accessible experimental range of momentum transfer. The original Lassettre series has been used very successfully for quantitative estimate of the dipole OS by extrapolating the measured GOS profile to zero momentum transfer. The other parameters f_n in the Lassettre series are related to linear combinations of the respective multipole matrix elements and can be used to characterize the nature of the underlying excitation [12,26]. For instance, the f_1 term has been shown to be related to the difference of the square of the quadrupole matrix element and the product of the dipole and octupole matrix elements [26]. For dipole or octupole-dominated transitions, the even coefficient, f_2, is found to have a positive sign while the odd coefficients, f_1 and f_3, are negative. The dipole OS, f_0, is always positive. In our earlier work on SF_6, we have shown that the higher order coefficients for a quadrupole-allowed S 2p transition appear to reverse in sign relative to the corresponding coefficients for a dipole-allowed S 2p transition [1]. For dipole-allowed transitions and/or non-dipole transitions dominated by a strong zero momentum-transfer component [10], these coefficients may be used to qualitatively describe the overall shapes of the GOS profiles. In particular, the coefficients f_1 and f_2 are more effective in shaping the lower momentum-transfer part of the GOS profile than the higher order coefficients. Within the somewhat large uncertainty, Table 1 shows that the f_0 and f_n/f_0 ($n = 1$–3) parameters for the two Si 2p shape resonances are more similar in relative magnitude than the Si 2pσ^* resonance. This is also quite evident in Fig. 2, which depicts the generally sharper decrease in the GOS profile of the Si 2pσ^* resonance (Fig. 2a) relative to those of the Si 2p shape resonances (Fig. 2b,c). These differences could be largely attributed to the differences in the final states of the respective transitions. In particular, the 2e and $7t_2$ orbitals in SiF_4 can be regarded in effect as atomic Si 3d orbitals, unlike the $6a_1$ orbital which corresponds to 'molecular' antibonding σ^* overlap between the Si 3s and F 2p orbitals.

It is of interest to compare the GOS profile of the Si 2p pre-edge transition in SiF_4 with the GOS profiles of other σ^* resonances in analogous cage-like molecules, particular for those transitions with the initial state involving an inner-shell orbital of the central atom. Except for the S 2p $\rightarrow 6t_{1u}$

Table 1
Comparison of Lassettre parameters for the σ^*, e and t_2 resonances in SiF_4 and SF_6

Energy loss (eV)	Assignment	f_0[a]	f_1/f_0	f_2/f_0	f_3/f_0
106.4	Si 2p $\rightarrow 6a_1$ [5,8][b]	$0.051 \pm 4\%$	$-18.9 \pm 25\%$	$164.8 \pm 30\%$	$-509.5 \pm 63\%$
117.5	Si 2p $\rightarrow$ 2e	$0.155 \pm 3\%$	$-32.0 \pm 16\%$	$439.1 \pm 29\%$	$-2043.7 \pm 54\%$
132.5	Si 2p $\rightarrow 7t_2$	$0.488 \pm 3\%$	$-24.1 \pm 20\%$	$302.1 \pm 41\%$	$-1596.4 \pm 64\%$
173.0	S 2p $\rightarrow 6a_{1g}$ [1]	$0.059 \pm 7\%$	$-129.0 \pm 24\%$	$6108.1 \pm 48\%$	$-95744.8 \pm 70\%$
184.5	S 2p $\rightarrow 2t_{2g}$	$0.180 \pm 5\%$	$-124.7 \pm 15\%$	$5752.4 \pm 33\%$	$-88964.1 \pm 49\%$
196.3	S 2p $\rightarrow 4e_g$	$0.223 \pm 5\%$	$-123.1 \pm 18\%$	$5207.6 \pm 41\%$	$-73127.0 \pm 67\%$

[a] The quoted errors in the f_n parameters are obtained from the curve-fitting procedure only and should not be taken as the accuracy of the results.

[b] More precise values can be found for various transitions in the original references. In [5], Friedrich et al. attributed the features at 106.4, 117.5, and 132.5 eV to Si 2p $\rightarrow \sigma^*$ (3s), Si 2p $\rightarrow$ 'e', and Si 2p $\rightarrow$ 't_2', respectively.

transition in SF_6, which has been shown by us [1] (and later confirmed by Turci et al. [27]) as a quadrupole-like transition, all of the GOS profiles for inner-shell transitions reported to date have the characteristic dipole-allowed shape, i.e., a declining shape from the maximum at zero momentum transfer [1,11,14]. In particular, the GOS profile for the C 1s $\rightarrow$ 7a_1 (σ^* resonance) and 8t_2 transitions located at 290.0 eV in CCl_4 and indeed those for all the C 1s $\rightarrow \sigma^*$ (C–Cl) (LUMO) transitions in $CF_{4-n}Cl_n$ ($n = 1$–3) appear to follow the same general shape as the GOS profile of the Si 2p $\rightarrow$ 6a_1 transition (Fig. 2a) [11]. Perhaps a more interesting comparison can be made between SiF_4 and SF_6, particularly for the inner-shell transitions involving the 2p initial states of the central atoms. Fig. 3 shows our earlier results for the GOS profiles of the S 2pσ^* and shape resonances in SF_6 [1]. As noted by Turci et al. [27] [1], our original plots (shown in Fig. 2 of [1]) depict 'differential' GOSs at the stated transition energies. Although the original figure nicely demonstrates the main conclusions of [1], we have replotted our original data as absolute GOS profiles for the respective transitions to facilitate better comparison in the present context. (It should be noted that only simple scaling factors are needed for this conversion from differential GOS to spectral GOS for individual features.) In SF_6, the LUMO 6a_{1g} consists of antibonding σ^* overlap between the S 3s and F 2p atomic orbitals. The corresponding GOS profile for the S 2p $\rightarrow \sigma^*$(S–F) resonance with a half width at half maximum (HWHM) of

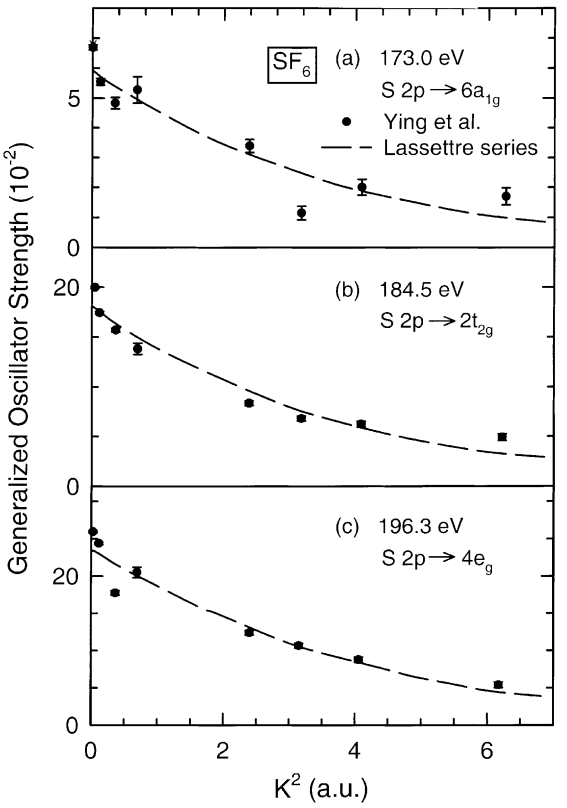

Fig. 3. Absolute GOS as a function of momentum transfer (K) squared for the S 2p features at (a) 173.0, (b) 184.5, and (c) 196.3 eV in SF_6 reported by Ying et al. [1]. The dashed lines correspond to semiempirical fits using the Lassettre series.

$K^2 \sim 2.3$ a.u. (Fig. 3a) is notably 'broader' [1] than that of the Si 2p $\rightarrow \sigma^*$(Si–F) resonance (Fig. 2a), with a HWHM of $K^2 \sim 0.7$ a.u. Indeed, similar observation can be made for the GOS profiles of the S 2p shape resonances in SF_6, both with HWHMs of $K^2 \sim 2.3$ a.u. (Fig. 3b,c), while the HWHMs for those of the corresponding Si 2p shape resonances in SiF_4 are $K^2 \sim 1.0$–1.2 a.u. (Fig. 2b,c). The smaller HWHMs for the GOS profiles of the SiF_4 features are consistent with the considerably smaller values for the f_1/f_0, f_2/f_0 and f_3/f_0 ratios relative to those for SF_6 (Table 1). These differences illustrate the sensitivity of the GOS profiles to the nature of the essentially atomic-like connecting states originated from the central atoms (Si in SiF_4 vs S in SF_6) in the inner-shell excitation processes.

[1] Despite the rather elaborate simulation schemes made by Turci et al. in [25] to try to explain the difference between their data and our SF_6 data reported in [1] in the large momentum-transfer region, we believe that such a discrepancy could be largely due to the relatively low impact energy (1.4 keV) employed by Turci et al. For inner-shell transitions (with large energy losses), it is well known that the breakdown of the Born approximation is more severe at lower impact energy and may indeed affect the premise of the GOS analysis (see, e.g., [13]). For our case (as in [1] and the present work), a considerably higher impact energy (2.5 keV) has been employed, and the accuracy of the GOS profiles obtained by our EELS apparatus has been reaffirmed recently by using widely accepted procedures as demonstrated in [15].

In summary, absolute GOS profiles of the prominent pre-edge σ^* resonance (Si $2p \rightarrow 6a_1$) and two post-edge shape resonances (Si $2p \rightarrow 2e$ and Si $2p \rightarrow 7t_2$) in the Si 2p shell of SiF_4 have been determined by using angle-resolved EELS at 2.5 keV impact energy. The GOS profiles of these Si 2p resonances are found to have a shape generally characteristic of predominantly dipole-allowed transitions, with the profile for the Si $2p\sigma^*$ resonance noticeably more sharply peaked at zero momentum transfer than the Si 2p shape resonances. The present work shows that despite the similarity in the general appearance of the measured GOS profiles, the subtle differences observed among the GOS profiles and between those of the corresponding transitions of other cage-like molecules (such as SF_6 [1] and CCl_4 [11]) underline the different nature of the contributing transitions from the inner-shell initial state to the respective final states. Quantitative calculations, together with an expanded data base of precise absolute GOS profiles, for these inner-shell transitions are clearly of great interest to provide further insights into the intricate inner-shell resonance processes of cage-like molecules.

Acknowledgements

This work was supported by the Natural Sciences and Engineering Research Council of Canada.

References

[1] J.F. Ying, C.P. Mathers, K.T. Leung, Phys. Rev. A 47 (1993) R5.
[2] J.F. Ying, T.A. Daniels, C.P. Mathers, H. Zhu, K.T. Leung, J. Chem. Phys. 99 (1993) 3390.
[3] J.D. Bozek, G.M. Bancroft, K.T. Tan, Chem. Phys. 145 (1990) 131, and references therein.
[4] W. Hayes, F.C. Brown, Phys. Rev. A 6 (1972) 21.
[5] H. Friedrich, B. Pittel, P. Rabe, W.H.E. Schwarz, B. Sonntag, J. Phys. B 13 (1980) 25.
[6] T.A. Ferrett, M.N. Piancaselli, D.W. Lindle, P.A. Heimann, D.A. Shirley, Phys. Rev. A 38 (1988) 701.
[7] R. Pűttner, M. Domke, K. Schulz, G. Kaindl, Chem. Phys. Lett. 250 (1996) 145.
[8] X. Guo, G. Cooper, W.-F. Chan, G.R. Burton, C.E. Brion, Chem. Phys. 161 (1992) 471.
[9] G.M. Bancroft, S. Aksela, H. Aksela, K.H. Tan, B.W. Yates, L.L. Coatsworth, J.S. Tse, J. Chem. Phys. 84 (1986) 5.
[10] X.W. Fan, K.T. Leung, J. Chem. Phys. 2001, in press.
[11] J.F. Ying, K.T. Leung, J. Chem. Phys. 101 (1994) 7311, and references therein.
[12] E.N. Lassettre, A. Skerbele, in: D. Williams (Ed.), Methods of Experimental Physics, vol. 3 (Part B), Academic, New York, 1974, p. 868.
[13] R.A. Bonham, in: C.R. Brundle, A.D. Baker (Eds.), Electron Spectroscopy: Theory Techniques and Applications, vol. 3, Academic, New York, 1979, p. 127.
[14] K.T. Leung, J. Electron Spectrosc. Relat. Phenom. 100 (1999) 237.
[15] X.W. Fan, K.T. Leung, Phys. Rev. A 62 (2000) 62703.
[16] M. Inokuti, Rev. Mod. Phys. 43 (1971) 297.
[17] M. Inokuti, J.L. Dehmer, T. Baer, J.D. Hanson, Phys. Rev. A 23 (1981) 95, and references therein.
[18] J.A. Wheeler, J.A. Bearden, Phys. Rev. 46 (1934) 755.
[19] A.E. Jonas, G.K. Schweitzer, F.A. Grimm, T.A. Carlson, J. Electron Spectrosc. Relat. Phenom. 1 (1972/73) 29.
[20] B.W. Yates, K.H. Tan, G.M. Bancroft, L.L. Coatsworth, J.S. Tse, J. Chem. Phys. 83 (1985) 4906.
[21] W.B. Perry, W.L. Jolly, J. Electron Spectrosc. Relat. Phenom. 4 (1974) 219.
[22] T.N. Olney, N.M. Cann, G. Cooper, C.E. Brion, Chem. Phys. 223 (1997) 59.
[23] E.N. Lassettre, J. Chem. Phys. 43 (1965) 4479.
[24] M.A. Dillon, E.N. Lassettre, J. Chem. Phys. 62 (1975) 2373.
[25] M.A. Dillon, M. Inokuti, Z.W. Wang, Radiat. Res. 102 (1985) 151.
[26] W.M. Huo, J. Chem. Phys. 71 (1979) 1593.
[27] C.C. Turci, J.T. Francis, T. Tyliszczak, G.G.B. de Souza, A.P. Hitchcock, Phys. Rev. A 52 (1995) 4678.